

# A ZZ Ceti white dwarf in SDSS J133941.11+484727.5

B.T. Gänsicke<sup>1</sup>, P. Rodríguez-Gil<sup>2</sup>, T.R. Marsh<sup>1</sup>, D. de Martino<sup>3</sup>, J. Nestoras<sup>4</sup>, P. Szkody<sup>5</sup>, A. Aungwerojwit<sup>1</sup>, S.C.C. Barros<sup>1</sup>, M. Dillon<sup>1</sup>, S. Araujo-Betancor<sup>2,6</sup>, M.J. Arévalo<sup>2,7</sup>, J. Casares<sup>2</sup>, P.J. Groot<sup>8</sup>, U. Kolb<sup>9</sup>, C. Lázaro<sup>2</sup>, P. Hakala<sup>10</sup>, I.G. Martínez-Pais<sup>2,7</sup>, G. Nelemans<sup>8</sup>, G. Roelofs<sup>8</sup>, M.R. Schreiber<sup>11,12</sup>, E. van den Besselaar<sup>8</sup>, C. Zurita<sup>2</sup>

<sup>1</sup> Department of Physics, University of Warwick, Coventry CV4 7AL, UK

<sup>2</sup> Instituto de Astrofísica de Canarias, 38200 La Laguna, Tenerife, Spain

<sup>3</sup> INAF - Osservatorio di Capodimonte, Via Moiariello 16, 80131 Napoli, Italy

<sup>4</sup> Department of Physics, Section of Astrophysics, Astronomy & Mechanics, University of Thessaloniki, 541 24 Thessaloniki, Greece

<sup>5</sup> Astronomy Department, University of Washington, Seattle, WA98195, USA

<sup>6</sup> Space Telescope Science Institute, 3700 San Martin Drive, Baltimore, MD21218, USA

<sup>7</sup> Departamento de Astrofísica, Universidad de La Laguna, E-38206 La Laguna, Tenerife, Spain

<sup>8</sup> Department of Astrophysics, IMAPP, Radboud University Nijmegen, P.O. Box 9010, 6500 GL Nijmegen, The Netherlands

<sup>9</sup> Department of Physics and Astronomy, The Open University, Milton Keynes MK7 6AA, UK

<sup>10</sup> Observatory, University of Helsinki, PO Box 14, Helsinki, Finland

<sup>11</sup> Astrophysikalisches Institut Potsdam, An der Sternwarte 16, 14482 Potsdam, Germany

<sup>12</sup> Departamento de Física y Meteorología, Facultad de Ciencias, Universidad de Valparaíso, Gran Bretaña 644, Valparaíso, Chile

Accepted 2005. Received 2005; in original form 2005

## ABSTRACT

We present time-resolved spectroscopy and photometry of the cataclysmic variable (CV) SDSS J133941.11+484727.5 (SDSS 1339) which has been discovered in the Sloan Digital Sky Survey Data Release 4. The orbital period determined from radial velocity studies is 82.524(24) min, close to the observed period minimum. The optical spectrum of SDSS 1339 is dominated to 90% by emission from the white dwarf. The spectrum can be successfully reproduced by a three-component model (white dwarf, disc, secondary) with  $T_{\text{wd}} = 12\,500$  K for a fixed  $\log g = 8.0$ ,  $d = 170$  pc, and a spectral type of the secondary later than M8. The mass transfer rate corresponding to the optical luminosity of the accretion disc is very low,  $\simeq 1.7 \times 10^{-13} M_{\odot} \text{yr}^{-1}$ . Optical photometry reveals a coherent variability at 641 s with an amplitude of 0.025 mag, which we interpret as non-radial pulsations of the white dwarf. In addition, a long-period photometric variation with a period of either 320 min or 344 min and an amplitude of 0.025 mag is detected, which bears no apparent relation with the orbital period of the system. Similar long-period photometric signals have been found in the CVs SDSS J123813.73–033933.0, SDSS J204817.85–061044.8, GW Lib and FS Aur, but so far no working model for this behaviour is available.

**Key words:** Stars: individual: SDSS J133941.11+484727.5 – novae, cataclysmic variables – stars: oscillations – white dwarfs

## 1 INTRODUCTION

A major impact of the Sloan Digital Sky Survey (SDSS) on the study of cataclysmic variables (CVs) has been the discovery of more than 20 systems (by Data Release 4) in which the optical spectrum is dominated by the white dwarf and there is no spectral signature of the donor star (Szkody et al. 2002b, 2003, 2004, 2005). These characteristics strongly suggest that those CVs have very low mass transfer rates, low mass donors, and presumably very short orbital periods. Hence, these systems resemble the old, evolved CVs predicted by population models to exist in vast numbers near

the orbital period minimum (Kolb 1993; Howell et al. 1997). Whether or not their number agrees with the theoretical models remains to be determined as their orbital periods need to be measured, along with estimates of their distances and mass transfer rates.

SDSS J133941.11+484727.5 (henceforth SDSS 1339, Fig. 1), a CV discovered in Data Release 4 (Szkody et al. 2005), is characterised by a very strong contribution of the white dwarf in the optical spectrum, and a clear absence of the TiO absorption bands typical of a late-type main-sequence donor star in the red part of the spectrum.

**Table 1.** Log of the observations. Read-out times at the WHT, TNG, and Kryoneri were  $\sim 40$  s,  $\sim 10$  s and  $\sim 5$  s, respectively.

Date	UT	Obs	Filter/Grism	Exp.(s)	Frames
2005 Jan 02	06:04 – 06:58	WHT	R600B/R316R	600	6
2005 Jan 04	04:00 – 06:54	WHT	R600B/R316R	400	25
2005 Jan 05	04:08 – 07:10	WHT	R600B/R316R	400	26
2005 Jan 06	05:39 – 06:51	WHT	R600B/R316R	400	6
2005 Jan 07	04:40 – 06:59	WHT	R600B/R316R	400	20
2005 Apr 04	19:36 – 00:24	KY	Clear	70	215
2005 Apr 07	21:31 – 03:03	KY	Clear	70	250
2005 Apr 29	21:45 – 01:43	TNG	$g'$	20	432

Here we report detailed spectroscopic and photometric follow-up observations of SDSS 1339, which confirm a short orbital period, a very low mass transfer rate, and identify a pulsating ZZ Ceti-type white dwarf in this CV.

## 2 OBSERVATIONS

In 2004, the International Time Programme of the night-time telescopes at the European Northern Observatory has been awarded for the study of CVs identified in the SDSS, with the aim of improving our understanding of compact binary evolution. The observations of SDSS 1339 were carried out as part of this project.

### 2.1 Spectroscopy

Time-resolved spectroscopy of SDSS 1339 was obtained in January 2005 at the 4 m William Herschel Telescope (WHT) on La Palma (Table 1). The double-arm spectrograph ISIS was used equipped with the R600B grating and a  $4k \times 2k$  pixel EEV detector in the blue arm and the R316R grating and a  $4.5k \times 2k$  pixel Marconi detector in the red arm. A  $1.2''$  slit was used on both arms, providing a spectral resolution of  $\simeq 0.9 \text{ \AA}$  covering the ranges  $3600 - 5000 \text{ \AA}$  and  $6100 - 8900 \text{ \AA}$ . The target exposures were interleaved with arc lamp and flat-field exposures to correct the wavelength scale for instrument flexure and to remove CCD fringing in the red arm. Spectra of the spectroscopic standard star Feige 34 were obtained on each night immediately after the observations of SDSS 1339. The standard reduction of the spectra, consisting of de-biasing, flat-fielding, optimal extraction and wavelength and flux calibration, was carried out using *Figaro* within the STARLINK suite and the *Pamela/Molly* packages. The average of the blue and red spectra (Fig. 2) is qualitatively similar to the SDSS spectrum (Szkody et al. 2005), clearly dominated by the broad Balmer absorption lines from the white dwarf photosphere. No noticeable signature of the companion star is detected in the red end of the spectrum. The Balmer emission lines are double-peaked, as typically observed in the quiescent spectra of short-period dwarf novae with moderate orbital inclinations. The emission lines of He I are very weak.

### 2.2 Photometry

Filterless CCD photometric time-series of SDSS 1339 were obtained in April 2005 at the 1.2 m Kryoneri telescope using

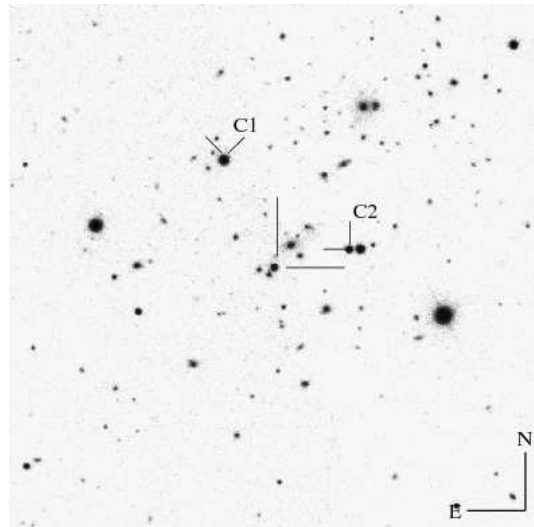


**Figure 1.**  $5' \times 5'$  finding chart of SDSS 1339 obtained from SDSS imaging data. Primary and secondary comparison stars for the CCD photometry are labelled ‘C1’ ( $g' = 16.7$ ) and ‘C2’ ( $g' = 18.5$ ).

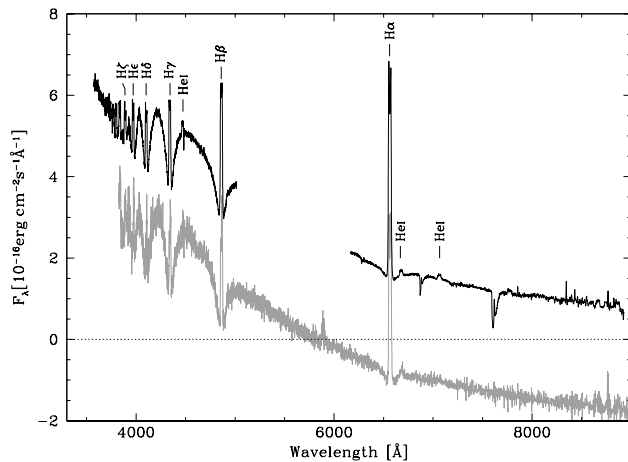


**Figure 2.** Average WHT/ISIS spectra of SDSS 1339 (black) and the SDSS discovery spectrum (gray, offset downwards by two flux units). Noticeable emission lines are identified. The broad Balmer absorption lines reflect the dominant contribution of the white dwarf to the optical flux.

a Photometrics SI-502  $516 \times 516$  pixel camera (Table 1). The object images were corrected for bias, dark current and flat field structures within MIDAS. Subsequently, the SEXTACTOR package (Bertin & Arnouts 1996) was used to perform aperture photometry on the processed images. The differential light curves of SDSS 1339 were computed relative to the comparison star ‘C1’ ( $g' = 16.7$ ), and a second comparison star ‘C2’ ( $g' = 18.5$ ) was used to verify that ‘C1’ is not variable and to monitor changes in the observing conditions. The Kryoneri light curves (Fig. 3, top panel) gave some evidence for short-term variability, and power spectra computed from both nights contained a signal near  $135 \text{ d}^{-1}$  ( $\simeq 10.7 \text{ min}$ ). Prompted by this discovery, we obtained additional  $g'$ -band CCD photometry at the 3.6 m Telescopio Nazionale Galileo (TNG) using DOLORES equipped with a

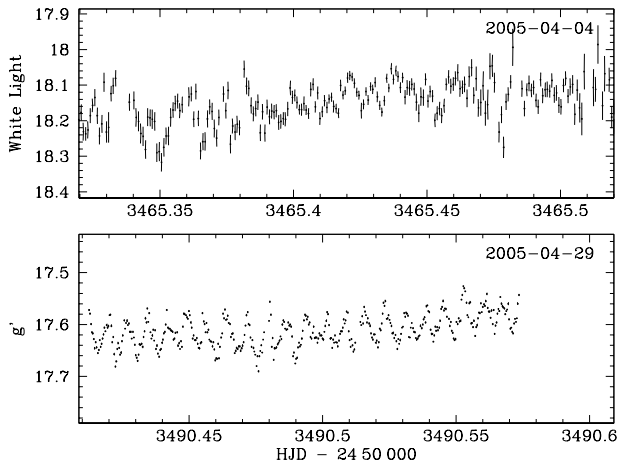


**Figure 3.** Kryoneri (top) and TNG (bottom) light curves of SDSS 1339. The average brightness of the TNG data agrees with the  $g'$ -band measurement from SDSS. The Kryoneri data were obtained in white light, the difference in mean magnitude is likely due to colour differences between the target and the comparison star.

Loral  $2k \times 2k$  pixel CCD. The CCD was binned  $2 \times 2$  and windowed in order to reduce the readout time. The TNG data were reduced in the same manner as described above, and the light curve (Fig. 3, lower panel) clearly confirms the presence of photometric variability at a period of  $\sim 10$  min.

### 3 SYSTEM PARAMETERS

#### 3.1 The orbital period

In order to determine the orbital period of SDSS 1339 from a radial velocity study, we applied heliocentric corrections to all spectra and binned them onto a homogeneous wavelength scale. The radial velocity variation of the  $H\alpha$  emission line wings were then measured using the double-Gaussian convolution technique described by Schneider & Young (1980) with a full width at half maximum of the individual Gaussians of  $200 \text{ km s}^{-1}$  and a separation of  $1500 \text{ km s}^{-1}$ . The strongest signal in the Scargle (1982) periodogram computed from the radial velocity data (Fig. 4) is detected at a period of  $82.524(24)$  min, where the error has been determined by fitting a sine wave to the radial velocity data. A fake data set constructed from a sine wave sampled at the same times of the observations, with a period of  $82.524$  min, and amplitude and error distribution similar to the observed radial velocities results in a nearly identical periodogram, confirming that the relatively complex structure of the periodogram is due to the temporal sampling of our spectroscopic data. We interpret this period as the orbital period of SDSS 1339. Folding the  $H\alpha$  radial velocity measurements over the orbital period produces a quasi-sinusoidal curve. A sine fit gives an amplitude of  $39 \pm 2 \text{ km s}^{-1}$  and a  $\gamma$ -velocity of  $8 \pm 1 \text{ km s}^{-1}$  (Fig. 5). We determine the orbital ephemeris

$$T_0 = \text{HJD } 2453372.74861(37) + 0.057309(17) \times E \quad (1)$$

from the sine fit to the radial velocity measurements, where  $T_0$  is the time of inferior conjunction of the secondary star if the radial velocity variation of the line wings traces the

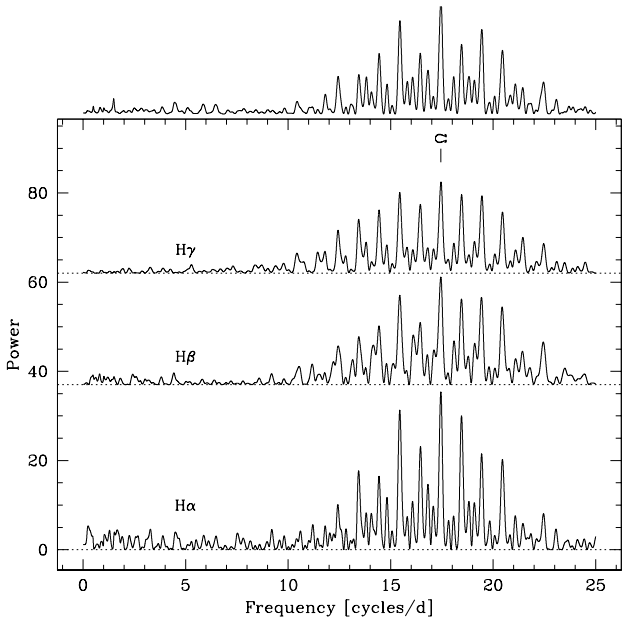


**Figure 4.** Main panel: Scargle periodograms computed from the radial velocity variations of the  $H\alpha$  (bottom curve),  $H\beta$  (middle curve) and  $H\gamma$  (top curve) line wings in SDSS 1339. The implied orbital period is  $P_{\text{orb}} = 82.524$  min. Top Panel: Scargle periodogram of a set of fake radial velocity data computed from a sine wave with  $P = 82.524$  min with the same temporal sampling as the observed data.

motion of the white dwarf. We caution, however, this interpretation, as the signal in the line wings is likely to be contaminated to some extent by the bright spot where the mass transfer stream from the secondary impacts the accretion disc. The same method was applied to the emission lines of  $H\beta$  and  $H\gamma$ , and resulted in consistent values for  $P_{\text{orb}}$ , though with larger errors as a consequence of the lower signal-to-noise ratio and the larger disturbance due to the white dwarf absorption lines in these lines compared to  $H\alpha$  (Fig. 4). Sine-fits to the radial velocities of  $H\beta$  and  $H\gamma$  give amplitudes of  $47 \pm 3 \text{ km s}^{-1}$  and  $60 \pm 5 \text{ km s}^{-1}$ , respectively and  $\gamma$ -velocities of  $1 \pm 2 \text{ km s}^{-1}$  and  $8 \pm 3 \text{ km s}^{-1}$ , respectively.

Figure 6 shows trailed spectrograms for  $H\gamma$ ,  $\text{He I } \lambda 4471$ ,  $H\beta$ , and  $H\alpha$  folded on 20 phase bins, using our ephemeris. The double-peaked profiles of  $H\alpha$ ,  $H\beta$  and  $H\gamma$  are apparent, with a half-separation of  $\sim 500 \text{ km s}^{-1}$ . There is a prominent S-wave whose semi-amplitude is consistent with this value, indicating an origin in the outer edge of the disc, very likely the bright spot. The half-separation of the double-peaked profiles together with the absence of eclipses in the light curves suggest an intermediate inclination. The absence of a photometric modulation that could be ascribed to the bright spot suggests that the bright spot contributes primarily in the Balmer emission lines. From the trailed spectra, it appears that the relative contribution of the bright spot increases for the higher members of the Balmer series, implying a stronger Balmer decrement in the disc compared to the bright spot.

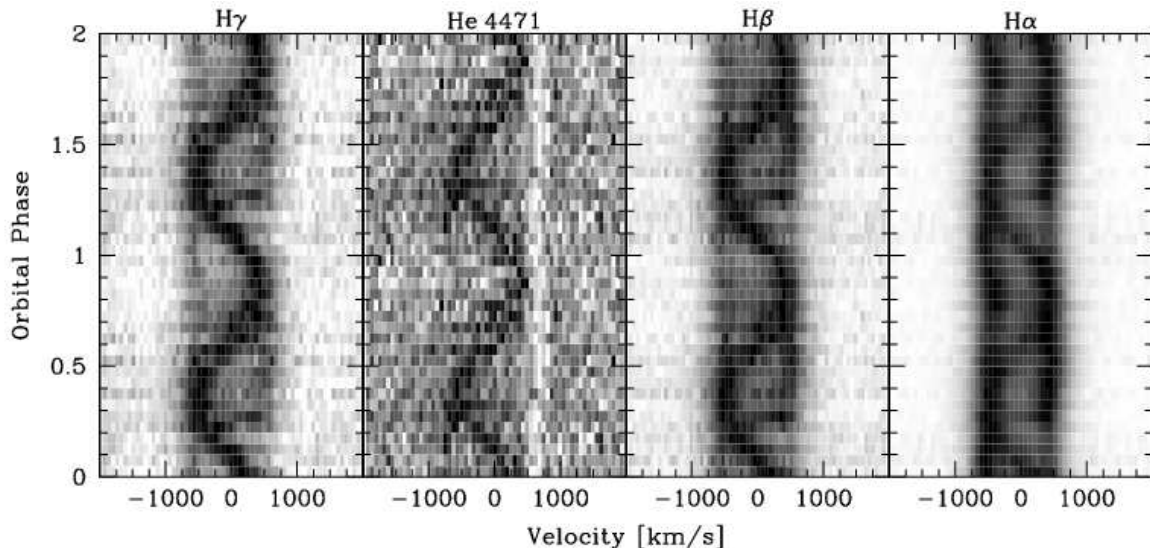


**Figure 6.** Trailed spectrograms of H $\gamma$ , He I  $\lambda$  4471, H $\beta$ , and H $\alpha$  folded on the orbital period of 82.524 min. The data are repeated over two cycles for clarity.

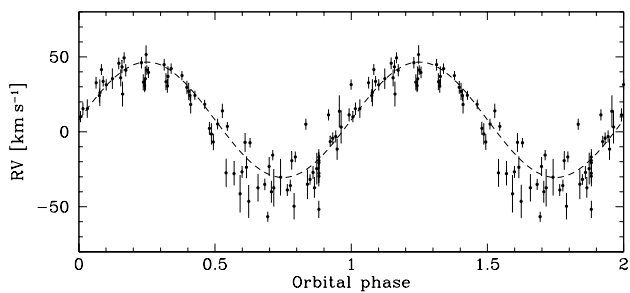


**Figure 5.** Radial velocity (RV) variation of H $\alpha$  measured from the time-resolved WHT spectroscopy of SDSS 1339 (Table 1), folded over the orbital period. The data are repeated over two cycles for clarity.

### 3.2 Additional system parameters

We have modelled the average WHT spectrum of SDSS 1339 as the sum of three individual components: the white dwarf, the accretion disc, and the donor star. The white dwarf is represented by synthetic spectra computed with Hubeny & Lanz (1995)’s TLUSTY/SYNPEC codes. We generated a grid of pure-hydrogen models covering the range 8000 K–20 000 K with the surface gravity fixed to  $\log g = 8.0$  ( $M_{\text{wd}} \simeq 0.6 M_{\odot}$ ). For the white dwarf radius, we assume  $R_{\text{wd}} = 8.7 \times 10^8$  cm following the Hamada & Salpeter (1961) mass-radius relation for zero-temperature carbon-oxygen white dwarfs. The accretion disc is represented by the emission of an isothermal and isobaric hydrogen slab, following the description by Gänsicke et al. (1997, 1999). The secondary star is represented by observed templates covering M0.5 to M9 from Beuermann et al. (1998) and L0 to L8 from

Kirkpatrick et al. (1999) and Kirkpatrick et al. (2000). We fix the radius of the secondary star to  $R_2 = 8.6 \times 10^9$  cm, corresponding to a  $M_2 = 0.08 M_{\odot}$  donor star at the low-mass end of the main sequence (the Roche-lobe radius of the secondary for this choice of  $M_2$  at the given orbital period).  $R_2$  obviously depends on the choice of  $M_2$  (and fairly little on  $M_{\text{wd}}$ , which was fixed to  $0.6 M_{\odot}$ , as stated above), but given that the spectral type-mass relation for CV donors at such low masses is undetermined we consider this a justified simplification.

Our approach is a forward-modelling rather than a fitting, and proceeds as follows. Free parameters are the white dwarf temperature  $T_{\text{wd}}$ , the distance  $d$  to SDSS 1339, the temperature  $T_{\text{d}}$  and column density  $\Sigma_{\text{d}}$  of the disc, and the spectral type of the secondary star Sp(2). As a first step, the disc spectrum for a given choice of  $(T_{\text{d}}, \Sigma_{\text{d}})$  is normalised to the observed flux of H $\alpha$ . The second step consists of choosing  $T_{\text{wd}}$  and adjusting the flux scaling factor of the model spectrum in a way that the sum of disc plus white dwarf fits the observed flux level in the spectrum from the blue arm. At this stage, the distance is determined by the knowledge of  $R_{\text{wd}}$  and the flux scaling factor, and the spectrum of a secondary star of spectral type Sp(2) is added to the model, scaled appropriately for  $R_2$  and  $d$ . This procedure is optimised until (a) the white dwarf model adequately reproduces the observed Balmer absorption lines, (b) the disc emission reproduces the observed emission line flux ratios, (c) the flux contribution from the secondary is sufficiently low to be consistent with the non-detection of molecular absorption bands in the red arm spectrum, and (d) the overall slope of the observed continuum is reproduced. The best-matching set of parameters is found to be  $T_{\text{wd}} = 12\,500$  K,  $T_{\text{d}} = 6600$  K,  $\Sigma_{\text{d}} = 1.7 \times 10^{-2}$  g cm $^{-2}$ ,  $d = 170$  pc, and Sp(2) later than M8. The luminosity of the accretion disc is  $\simeq 10^{30}$  erg s $^{-1}$ , less than 10% of the white dwarf luminosity. For an assumed white dwarf mass of  $0.6 M_{\odot}$ , this luminosity corresponds to an accretion rate of  $\dot{M} \simeq 1.7 \times 10^{-13} M_{\odot}$  yr $^{-1}$ . A caveat to white dwarf temperature

and distance determination is the unknown mass of the primary. Masses of single white dwarfs (e.g. Koester et al. 1979; Bergeron et al. 1992; Liebert et al. 2005) are predominantly clustered sharply around  $\sim 0.6 M_{\odot}$ . The standard method used for single white dwarfs, modelling the Balmer absorption lines, is not available for CV white dwarfs due to contamination by the accretion disc/stream and the secondary star, and white dwarf mass estimates have to be determined from radial velocity studies, eclipse timing, or ultraviolet spectral modelling. Consequently, the number of CVs with undisputed mass measurements is very small. The secular evolution of CV white dwarf masses depends on the ratio of accreted material to material ejected during classical nova eruptions, and the exact details are not very well established (Yaron et al. 2005). In the light of the uncertain mass of the white dwarf in SDSS 1339, we have therefore repeated the above analysis assuming a white dwarf mass higher (lower) by  $0.3 M_{\odot}$  and find a white dwarf effective temperature higher (lower) by  $\simeq 500 - 1000$  K and a distance lower (larger) by  $\simeq 35$  pc.

If we assume that the disc emission is all what there is in terms of accretion luminosity, the implied accretion rate is very low, in fact, much lower than mass transfer rates predicted from angular momentum loss via gravitational radiation,  $\simeq 3.5 \times 10^{-11} M_{\odot} \text{ yr}^{-1}$  for a  $0.6 M_{\odot}$  white dwarf. Some additional accretion luminosity may be released in X-rays. The ROSAT All Sky Survey (Voges et al. 2000) contains a faint source, 1RXS J133941.9+484844, with  $1.23 \pm 0.56 \times 10^{-2}$  cts  $\text{s}^{-1}$ , that within its large positional uncertainty ( $77.4''$ ) coincides with SDSS 1339. A pointed observation of that region led to the detection of 2RXP J133938.5+484722, with  $1.5 \times 10^{-2}$  cts  $\text{s}^{-1}$ . No error on the position and count rate are given in the *The Second ROSAT Source Catalog of Pointed Observations*. It is possible that both X-ray sources are identical, and that SDSS 1339 is the optical counterpart. If the X-rays detected by ROSAT are indeed associated with SDSS 1339, the observed PSPC count rate corresponds to an unabsorbed bolometric flux of of  $\sim 2 \times 10^{-13}$  erg  $\text{cm}^{-2} \text{ s}^{-1}$ , assuming a thermal Bremsstrahlung spectrum with  $2 \text{ keV} \lesssim kT \lesssim 5 \text{ keV}$ , as typically observed in short-period CVs, and a neutral hydrogen column density of  $N_{\text{H}} = 1.1 \times 10^{20} \text{ cm}^{-2}$ . For  $d = 170$  pc, the implied X-ray luminosity would be  $\sim 10^{30}$  erg  $\text{s}^{-1}$ , very similar to the optical accretion luminosity derived above, and comparable to the X-ray emission of the well-studied minimum period CV WZ Sge (Mukai & Patterson 2004). A deeper X-ray observations is clearly desirable to test whether SDSS 1339 is the source of the X-rays detected by ROSAT.

In summary, in SDSS 1339 the accretion disc contributes less than 10% of the optical light, which is very low compared to other short-period CVs, and may have an X-ray flux comparable to that of WZ Sge, suggesting a very low accretion rate. A low mass transfer rate from the secondary is also supported by the absence of the signature from a bright spot in the light curve (Fig. 3, see also Fig. 8). The current data suggest that the mass transfer from the secondary is lower than that predicted by gravitational radiation. Following Townsley & Bildsten (2003), the white dwarf temperature can be used as an estimate of the secular mean of the accretion rate, and it appears that the white dwarf in SDSS 1339 is not unusually cold compared to other CVs near the orbital minimum. In fact, its temperature is well

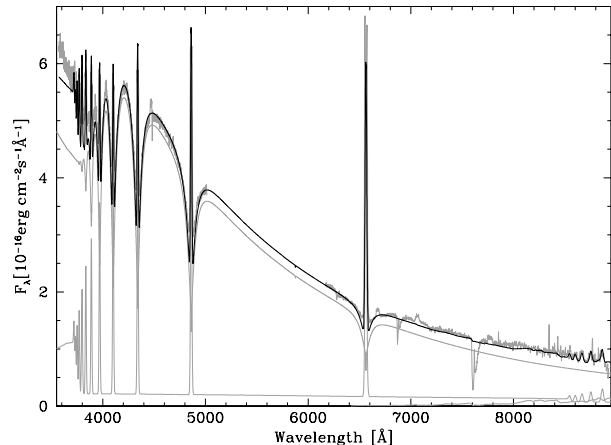


**Figure 7.** Three-component model (white dwarf, optically thin disc, secondary star) of the average WHT spectrum of SDSS 1339. The observed data as well as the three individual components are plotted as gray lines, the summed model as a black line. The parameters are  $T_{\text{wd}} = 12\,500$  K (assuming  $\log g = 8.0$ ),  $T_{\text{d}} = 6600$  K,  $\Sigma_{\text{d}} = 1.7 \times 10^{-2} \text{ g cm}^{-2}$ ,  $\text{Sp}(2) = \text{M8}$ , and  $d = 170$  pc.

in line with the predictions for  $\dot{M}$  from gravitational radiation. A possible solution to the discrepancy between the accretion rate estimated from the optical emission of the accretion disc (and the possible X-ray component) is that the system is currently accreting below its secular mean rate.

#### 4 A ZZ CETI-TYPE WHITE DWARF

The power spectra computed from the Kryoneri and TNG photometric data consistently contain a strong signal at  $134.61 \text{ d}^{-1}$  (Fig. 8). Given the estimated temperature of the white dwarf, the most obvious explanation for this signal are non-radial pulsations with a period of  $P = 641.84$  s. The amplitude of the pulsation is  $\simeq 0.025$  mag, which is well within the range observed in single ZZ Ceti white dwarfs (Winget 1998). Figure 9 shows the TNG photometry folded over the pulse period of 641.84 s, after subtracting a long-period photometric modulation with  $P = 344.32$  min (see Sect. 5). The detection of pulsations makes SDSS 1339 only the eighth pulsating white dwarf in a CV.

The fact that only one pulsation mode is detected above a  $3\text{-}\sigma$  threshold raises the question whether other mechanisms than non-radial pulsations could cause the observed variability. In principle, the white dwarf spin could account for a stable clock in photometric data, as seen in intermediate polars. However, in intermediate polars, multiple optical modulations are observed, usually at the white dwarf rotational period, the orbital period and sideband periods. In these systems the spin modulation stems the reprocessing of X-rays in the magnetically confined accretion flow onto the WD while the orbital and the beat periodicities are due to reprocessing in the accretion disc and the bright spot. However, in SDSS 1339 we do not detect a significant signal at the orbital period, nor any beat signal. Furthermore, the optical spectrum of SDSS 1339 in no way resembles that of any confirmed intermediate polar, as it has literally no  $\text{He II } \lambda 4686$  emission, and not a single intermediate polar is

known whose optical emission is dominated by the white dwarf. The non-detection of Zeeman splitting in the Balmer lines, specifically the higher members, limits the possible field strength of the white dwarf to  $B < 1$  MG. Finally, as discussed above, SDSS 1339 is not a prominent X-ray source.

## 5 A LONG NON- $P_{\text{orb}}$ PHOTOMETRIC PERIODICITY

Inspection of the power spectra (Fig. 8) reveals a low-frequency signal of variable amplitude in all three nights. The power spectrum of the combined data contains two signals of nearly identical amplitude at  $4.50 \text{ d}^{-1}$  and  $4.18 \text{ d}^{-1}$ , with the latter one being the stronger peak. Removing the photometric data with the 641.84 s pulse signal and fitting them to a sine wave results in two possible periods, 319.95(5) min or 344.32(7) min. Figure 10 shows the pulse-removed photometry folded over 344.32 min. The average amplitude of this modulation is 0.025 mag, but the power spectra indicate that the amplitude is rather variable on a time scale of days. No equivalent long-period variability is detected in the radial velocity variations (Sect. 3.1).

Long-period photometric modulations with periods in the range 7–12 h have been reported for SDSS J123813.73–033933.0 and SDSS J204817.85–061044.8 (Zharikov et al. 2005; Woudt et al. 2005), which are both short-period CVs with white-dwarf dominated optical spectra. A similar phenomenon is also well-documented in GW Lib, where a 125.4 min photometric modulation has been detected with an amplitude of  $\simeq 0.05$  mag on several occasions (Woudt & Warner 2002). In FS Aur, a 205.5 min photometric modulation with a 0.24 mag amplitude was detected by Tovmassian et al. (2003). In both systems, the photometric modulations occur on periods substantially longer than the orbital periods (76.9 min and 85.7 min, respectively). Tovmassian et al. (2003) invoke the precession of a rapidly rotating white dwarf as a possible explanation for the long-period signal found in FS Aur. To date, this hypothesis could not be confirmed, and no other plausible model has been suggested.

The puzzle of long-period signals in short-period CVs is exacerbated by the case of HS 2331+3905, where a *spectroscopic* (i.e. radial velocity) periodicity of  $\sim 3.5$  h is found that is in no way associated with the 81.1 min orbital period of the system, and that does not have any photometric equivalent (Araujo-Betancor et al. 2005). Whereas there is mounting evidence that variability on periods much longer than the orbital period is fairly common among CVs near the minimum period, the origin of this phenomenon is unclear.

## 6 DISCUSSION

Asteroseismology of single white dwarfs is a well-established field, with close to 100 ZZ Ceti stars known (more than half of which were discovered in the SDSS, Mukadam et al. 2004; Mullally et al. 2005). Winget (1998) and Clemens (1993) note a substantial diversity of the single pulsating ZZ Ceti stars as a function of their temperature. The hot ( $T_{\text{wd}} \simeq 12000$  K) pulsators have a relatively small number

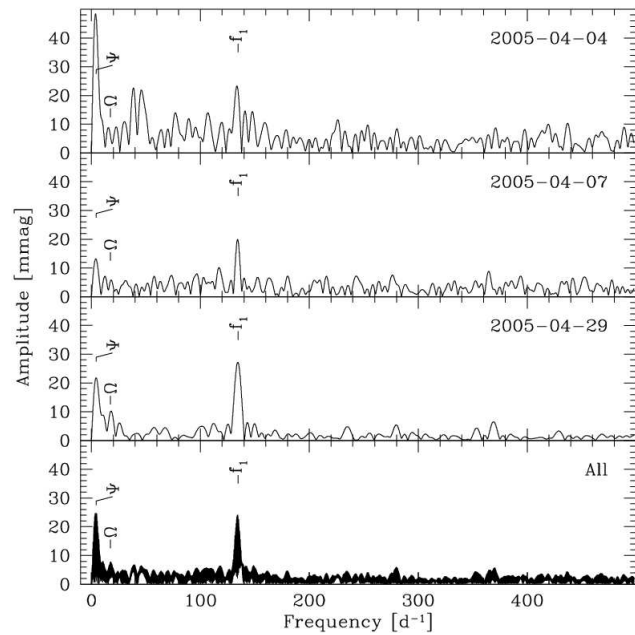


**Figure 8.** Power spectra computed from the three individual nights of photometry obtained at Kryoneri Observatory and with the TNG, and from the combined data.  $f_1$  and  $\Psi$  indicate the frequencies of the white dwarf pulsation (641.84 s) and a photometric modulation of unknown nature (319.95 min or 344.32 min). No significant signal is detected in the power spectra at the orbital period  $\Omega$  (82.524 min).

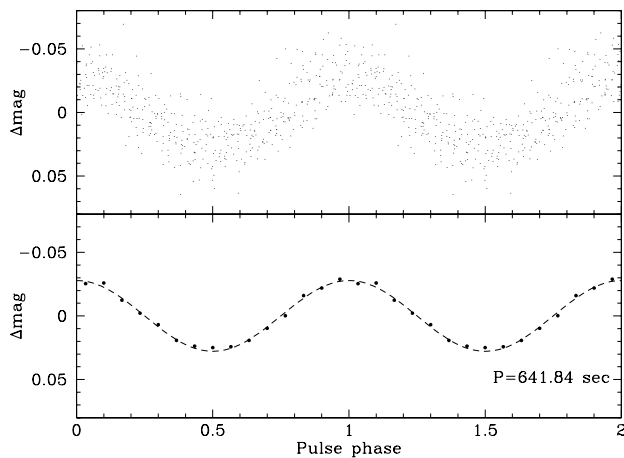


**Figure 9.** Pulse-folded light curves of SDSS 1339, assuming  $P = 641.84$  s. The long-period 344.32 min modulation (Sect. 5) has been removed. Top panel: all data points from the TNG. Bottom panel: TNG data binned into 15 phase slots. Plotted as dashed line is a sine fit to the binned and folded data. The data are repeated over two cycles for clarity.

of modes, typically in the range 100–300 s, with a high degree of stability both in frequencies and amplitudes. In contrast to this, the cooler ( $T_{\text{wd}} \simeq 11000$  K) pulsators are characterised by longer periods in the range 600–1000 s, larger amplitudes, more modes, and what appears to be unstable amplitudes of the individual modes. Overall, the power

**Table 2.** Properties of pulsating white dwarfs in cataclysmic variables

System	$P_{\text{orb}}$ [min]	Mag	periods [s]	Outbursts	$T_{\text{wd}}$ [K] / $\log g$	Ref
PQ And	80.7/78.5 <sup>p</sup>	$V \simeq 19.1$	1263, 634	1938, 1967, 1988	12 000/7.7 <sup>a</sup>	1,2,3
GW Lib	76.8 <sup>s</sup>	$V \simeq 16.7^b$	650, 370, 230	1983	11 000/8.0 <sup>c</sup> 14 700/8.0 <sup>d</sup>	4,5,6,7,8
HS 2331+3905	81.1 <sup>pe</sup>	$V \simeq 16.5$	310, 336, 419 <sup>e</sup>	-	10 500/8.0 <sup>f</sup>	9
RE J1255+266	119.4 <sup>p</sup>	$V \simeq 19.2$	668, 1236, 1344	1994	36 480/9.0 <sup>g</sup> 11 000–15 000 <sup>h</sup>	10,11,12
SDSS J013132.39-090122.3	98: <sup>s</sup>	$g' \simeq 18.3$	260, 335, 595	-	-	13,14
SDSS 133941.11+484727.5	82.5 <sup>s</sup>	$g' \simeq 17.6$	642	-	12 500/8.0 <sup>c</sup>	15, this paper
SDSS J161033.64-010223.3	80.5 <sup>p</sup>	$g' \simeq 19.1$	607, 345, 304, 221	-	-	15,16
SDSS J220553.98+115553.7	-	$g' \simeq 20.1$	330, 475, 575	-	-	13,14

<sup>1</sup>Schwarz et al. (2004), <sup>2</sup>Patterson et al. (2005a), <sup>3</sup>Vanlandingham et al. (2005), <sup>4</sup>Szkody et al. (2000), <sup>5</sup>Szkody et al. (2002a), <sup>6</sup>Thorstensen et al. (2002), <sup>7</sup>Thorstensen (2003), <sup>8</sup>van Zyl et al. (2004), <sup>9</sup>Araujo-Betancor et al. (2005), <sup>10</sup>Watson et al. (1996), <sup>11</sup>Wheatley et al. (2000), <sup>12</sup>Patterson et al. (2005b), <sup>13</sup>Szkody et al. (2003), <sup>14</sup>Warner & Woudt (2004), <sup>15</sup>Szkody et al. (2005), <sup>16</sup>Szkody et al. (2002b), <sup>17</sup>Woudt & Warner (2004).

: Uncertain estimate. <sup>p</sup> Photometric period. <sup>pe</sup> Photometric period, eclipsing. <sup>s</sup> Spectroscopic period. <sup>a</sup> Fit to the Balmer lines. <sup>b</sup> Downes et al. (2001) list a pre-outburst photometric magnitude of  $\simeq 18.5$ , however, most published pre- and post-outburst photometry suggests  $V \simeq 16.7$  (USNO, DENIS, Thorstensen 2003). <sup>c</sup> Fit to the Balmer lines with fixed  $\log g$ . <sup>d</sup> Fit to far-ultraviolet spectra with fixed  $\log g$ . <sup>e</sup> Very complex power spectrum. <sup>f</sup> Fit to far-ultraviolet/optical spectrum with fixed  $\log g$ . <sup>g</sup> Fit to the Balmer lines, using a model grid with  $20\,000\text{ K} \leq T_{\text{wd}} \leq 40\,000\text{ K}$ . <sup>h</sup> Estimated from *UBVI* colours.

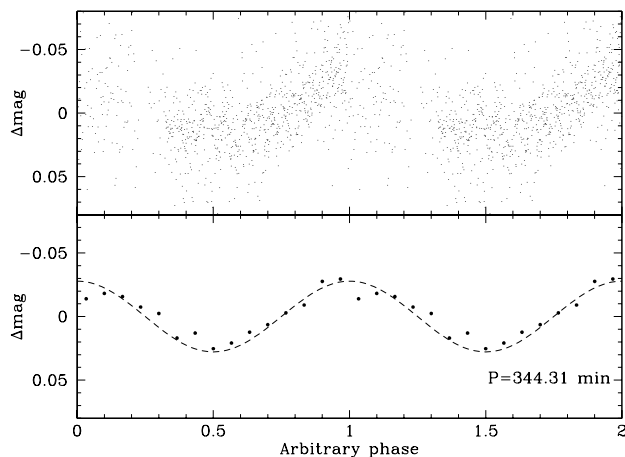


**Figure 10.** All photometric data (Kryoneri & TNG) folded over the photometric period of 344.32 min. The 641.84 s pulse period has been removed. Top panel: all individual data points. Bottom panel: Data binned into 15 phase slots. Plotted as a dashed line is a sine fit to the binned and folded data. The data are repeated over two cycles for clarity.

spectra of the cooler pulsators are much more challenging to interpret than those of the hotter ones.

Since the discovery of non-radial pulsations of the white dwarf in GW Lib (van Zyl et al. 2004), much effort has been invested in identifying additional CV white dwarf pulsators (e.g. Woudt & Warner 2004; Araujo-Betancor et al. 2005; Patterson et al. 2005b) and in theoretical modelling of accreting white dwarf pulsators (Townesley et al. 2004). The scientific potential of asteroseismology in CVs is enormous, as it could allow accurate measurements of white dwarf masses, envelope masses, rotation rates, and magnetic fields – important parameters for understanding the structure and evolution of CVs which are so far difficult or not at all measurable. From the current roster of known CV white dwarf pulsators given in Table 2, it is clear that there is still a long way to go before achieving these goals.

An observational problem is that the CV white dwarf

pulsators are all much fainter than the field ZZ Ceti stars, in fact, hardly any single white dwarf pulsator with  $V > 19$  has been studied. The need to detect low-amplitude variability in these objects requires photometry obtained at large-aperture telescopes, where it is difficult to obtain observing runs long enough to determine accurate pulsation frequencies. The largest photometric data sets have been published for the two brightest CV pulsators, GW Lib and HS 2331+3905 (van Zyl et al. 2004; Araujo-Betancor et al. 2005). Both systems exhibit large variations in their power spectra on time scales of days to months, and no detailed mode identification has been achieved so far.

A problem intrinsic to the nature of accreting sources is the determination of the white dwarf temperature. Using optical wavelengths alone gives rise to large systematic uncertainties as any fit to the Balmer absorption lines is subject to an unknown contribution from the accretion disc (and possibly the bright spot). Given how narrow the ZZ Ceti instability strip of single white dwarfs is in terms of temperature, there is little hope in empirically defining the equivalent for CV white dwarfs from optical data alone. A substantial improvement comes from far-ultraviolet (FUV) data, as the white dwarf dominates in this wavelength range, and both the Ly $\alpha$  absorption profile as well as the FUV to optical spectral energy distribution can be used in estimating the white dwarf temperature. Interestingly enough, again GW Lib and HS 2331+3905 are the only systems with accurate white dwarf temperatures, and the FUV data for GW Lib indicate that parameters might be very different in CV pulsators compared to field ZZ Ceti stars: the FUV-determined temperature is 14 700 K for an assumed  $\log g = 8.0^1$ , well outside the instability strip of single ZZ Ceti stars (Szkody et al. 2002a). Szkody et al. (2002a) note that the

<sup>1</sup> In contrast to single white dwarfs, it is very difficult if not impossible to break the degeneracy between  $T_{\text{wd}}$  and  $\log g$  that occurs in spectral modelling. The reason is that the Balmer lines are strongly contaminated by the accretion disc, and that the FUV observations provided by *HST*/STIS cover only the red wing of Ly $\alpha$ .

FUV spectrum is better fitted with a two-temperature white dwarf model, where the lower temperature gets fairly close to the hot edge of the ZZ Ceti instability strip. However, the physical origin of such an inhomogeneous temperature distribution over the white dwarf is not clear. HS 2331+3905 has a temperature just close to the cold edge of the ZZ Ceti instability strip, which is consistent with its very complex power spectrum (Araujo-Betancor et al. 2005).

Currently, all known CV white dwarf pulsators have orbital periods very close to the orbital period minimum (Table 2), where accretion rates are sufficiently low to correspond to white dwarf effective temperatures close to the ZZ Ceti instability strip. The immediate task in improving our understanding of the pulsations in accreting white dwarfs is now to measure accurate effective temperatures for all white-dwarf dominated CVs, establish whether or not they are pulsating, and determine their pulsation frequencies. Only once the pulsation modes have been identified, asteroseismology may reveal details about the structure of these stars.

## 7 CONCLUSIONS

We have determined the orbital period of SDSS 1339 to be 82.524 min from radial velocity studies. The optical spectrum is dominated by the white dwarf, and can be successfully modelled with a (12 500 K,  $\log g = 8.0$ ) synthetic spectrum. The contribution of the accretion disc to the observed optical flux is less than 10%, corresponding to a very low optical accretion luminosity of  $\simeq 1.7 \times 10^{-13} M_{\odot} \text{ yr}^{-1}$ . CCD photometry of SDSS 1339 reveals the presence of variability with a stable 641 s period and an amplitude of  $\simeq 0.025$  mag, which we interpret as non-radial pulsations of the white dwarf. Further photometric work is encouraged to probe for additional pulsation modes. Similar to several other short-period CVs, SDSS 1339 displays an apparently coherent photometric variability on time scales much longer than the orbital period. The nature of this variability is not understood.

## ACKNOWLEDGEMENTS

BTG and TRM were supported by a PPARC Advanced Fellowship and a PPARC Senior Fellowship. DdM acknowledges funding from the Italian Ministry of University and Research (MIUR). PS acknowledges some support from NSF grant AST 02-05875. AA thanks the Royal Society for generous funding. PJG, GR, EvdB are supported by NWO-VIDI grant 639.042.201 and GN is supported by NWO-VENI grant 639.041.405. MRSK thanks for supported by the Deutsches Zentrum für Luft- und Raumfahrt (DLR) GmbH under contract No. FKZ 50 OR 0404. Based in part on observations made with the William Herschel Telescope, which is operated on the island of La Palma by the Isaac Newton Group in the Spanish Observatorio del Roque de los Muchachos of the Instituto de Astrofísica de Canarias (IAC); on observations made with the Telescopio Nazionale Galileo operated on the island of La Palma by the Centro Galileo Galilei of the INAF (Istituto Nazionale di Astrofisica) at the Spanish Observatorio del Roque de los Muchachos of the IAC; and on observations made at the 1.2 m telescope, located

at Kryoneri Korinthias, and owned by the National Observatory of Athens, Greece. The WHT and TNG data were obtained as part of the 2004 International Time Programme of the night-time telescopes at the European Northern Observatory. We thank the referee for helpful comments.

## REFERENCES

- Araujo-Betancor, S., et al., 2005, *A&A*, 430, 629  
 Bergeron, P., Saffer, R. A., Liebert, J., 1992, *ApJ*, 394, 228  
 Bertin, E., Arnouts, S., 1996, *A&AS*, 117, 393  
 Beuermann, K., Baraffe, I., Kolb, U., Weichhold, M., 1998, *A&A*, 339, 518  
 Clemens, J. C., 1993, *Baltic Astronomy*, 2, 407  
 Downes, R. A., Webbink, R. F., Shara, M. M., Ritter, H., Kolb, U., Duerbeck, H. W., 2001, *PASP*, 113, 764  
 Gänsicke, B. T., Beuermann, K., Thomas, H. C., 1997, *MNRAS*, 289, 388  
 Gänsicke, B. T., Sion, E. M., Beuermann, K., Fabian, D., Cheng, F. H., Krautter, J., 1999, *A&A*, 347, 178  
 Hamada, T., Salpeter, E. E., 1961, *ApJ*, 134, 683  
 Hameury, J.-M., Lasota, J.-P., eds., 2005, *The Astrophysics of Cataclysmic Variables and Related Objects*, ASP Conf. Ser. 330  
 Howell, S. B., Rappaport, S., Politano, M., 1997, *MNRAS*, 287, 929  
 Hubeny, I., Lanz, T., 1995, *ApJ*, 439, 875  
 Kirkpatrick, J. D., et al., 1999, *ApJ*, 519, 802  
 Kirkpatrick, J. D., et al., 2000, *AJ*, 120, 447  
 Koester, D., Schulz, H., Weidemann, V., 1979, *A&A*, 76, 262  
 Kolb, U., 1993, *A&A*, 271, 149  
 Liebert, J., Bergeron, P., Holberg, J. B., 2005, *ApJS*, 156, 47  
 Mukadam, A. S., et al., 2004, *ApJ*, 607, 982  
 Mukai, K., Patterson, J., 2004, in *Tovmassian, G., Sion, E., eds., Compact Binaries and Beyond*, no. 20 in Conf. Ser., RMAA, p. 244  
 Mullally, F., Thompson, S. E., Castanheira, B. G., Winget, D. E., Kepler, S. O., Eisenstein, D. J., Kleinman, S. J., Nitta, A., 2005, *ApJ*, 625, 966  
 Patterson, J., Thorstensen, J., Armstrong, E., Henden, A., Hynes, R., 2005a, *PASP*, in press (astro-ph/0506135)  
 Patterson, J., Thorstensen, J. R., Kemp, J., 2005b, *PASP*, 117, 427  
 Scargle, J. D., 1982, *ApJ*, 263, 835  
 Schneider, D. P., Young, P., 1980, *ApJ*, 240, 871  
 Schwarz, G. J., Barman, T., Silvestri, N., Szkody, P., Starrfield, S., Vanlandingham, K., Wagner, R. M., 2004, *PASP*, 116, 1111  
 Szkody, P., Desai, V., Hoard, D. W., 2000, *AJ*, 119, 365  
 Szkody, P., Gänsicke, B. T., Howell, S. B., Sion, E. M., 2002a, *ApJ Lett.*, 575, L79  
 Szkody, P., et al., 2002b, *AJ*, 123, 430  
 Szkody, P., et al., 2003, *AJ*, 126, 1499  
 Szkody, P., et al., 2004, *AJ*, 128, 1882  
 Szkody, P., et al., 2005, *AJ*, 129, 2386  
 Thorstensen, J. R., 2003, *AJ*, 126, 3017  
 Thorstensen, J. R., Patterson, J., Kemp, J., Vennes, S., 2002, *PASP*, 114, 1108  
 Tovmassian, G., et al., 2003, *PASP*, 115, 725



- Townsley, D. M., Bildsten, L., 2003, *ApJ Lett.*, 596, L227  
Townsley, D. M., Arras, P., Bildsten, L., 2004, *ApJ Lett.*, 608, L105  
van Zyl, L., et al., 2004, *MNRAS*, 350, 307  
Vanlandingham, K. M., Schwarz, G. J., Howell, S. B., 2005, *pasp*, in press (astro-ph/0506098)  
Voges, W., et al., 2000, *IAU Circ.*, 7432  
Warner, B., Woudt, P., 2004, in Kurtz, D. W., Pollard, K. R., eds., *Variable Stars in the Local Group*, ASP Conf. Ser. 310, p. 392  
Watson, M. G., Marsh, T. R., Fender, R. P., Barstow, M. A., Still, M., Page, M., Dhillon, V. S., Beardmore, A. P., 1996, *MNRAS*, 281, 1016  
Wheatley, P. J., Burleigh, M. R., Watson, M. G., 2000, *MNRAS*, 317, 343  
Winget, D. E., 1998, *Journal of the Physics of Condensed Matter*, 10, 11247  
Woudt, P. A., Warner, B., 2002, *Ap&SS*, 282, 433  
Woudt, P. A., Warner, B., 2004, *MNRAS*, 348, 599  
Woudt, P. A., Warner, B., Pretorius, M. L., Dale, D., 2005, in Hameury & Lasota (2005), p. 325, p. 325  
Yaron, O., Prialnik, D., Shara, M. M., Kovetz, A., 2005, *ApJ*, 623, 398  
Zharikov, S. V., Tovmassian, G. H., Neustroev, V., Michel, R., Napiwotzki, R., 2005, in Hameury & Lasota (2005), p. 327, p. 327

This paper has been typeset from a  $\text{\TeX}$ / $\text{\LaTeX}$  file prepared by the author.